QCD coherence in high-energy reactions

Yu. L. Dokshitzer, V. A. Khoze, and S. I. Troyan

Academy of Sciences of the Union of Soviet Socialist Republics, Leningrad Nuclear Physics Institute, SU-188350 Gatchina, Leningrad District, Union of Soviet Socialist Republics

A. H. Mueller

Department of Physics, Columbia University, New York, New York 10027

The authors review the ideas and manifestations of QCD coherence in high-energy reactions producing jets. They suggest experiments involving two-jet production, high-$p_\perp\gamma$ production and high-$p_\perp W$ production at hadronic colliders as ways to see QCD coherence in stringlike effects. They also suggest a procedure for finding the dip in the inclusive hadron spectrum of jets for those jets produced at hadron colliders. Simple explanations of the various coherence effects in QCD are discussed, as is the idea of local parton-hadron duality.

CONTENTS

I. INTRODUCTION

The existence of hadron jets is the most striking success of QCD. These jets were definitively first seen in 1975 (Hanson *et al.*, 1975), in e^+e^- collisions, and are now being intensively investigated at both e^+e^- and hadronic colliders. Hadronic jet physics will be one of the central problems of investigation for the e^+e^-, pp, and ep colliders of the future. Detailed studies of jets are necessary for better understanding and for testing of both perturbative and nonperturbative QCD, for designing detectors of the present and of the future, and for finding new heavy particles in high-energy reactions.

In the last few years hadron jet physics has reached a mature level of sophistication. At the partonic level, developments in QCD theory allow one to make testable quantitative predictions, with controllable accuracy, for jet characteristics in terms of analytical perturbative calculations (Bassetto *et al.*, 1983; Mueller, 1983, 1984; Dokshitzer and Troyan, 1984; Malaza and Webber, 1984; Azimov *et al.*, 1985b, 1985c, 1986a, 1986b; Gaffney and Mueller, 1985; Dokshitzer *et al.*, 1986; Malaza, 1986; Ciafaloni, 1987). At the same time there has been enormous progress in writing Monte Carlo simulations (Anderson *et al.*, 1983; Marchesini and Webber, 1984; Webber, 1984; Gottschalk, 1985; Sjostrand, 1985, 1986; Field, 1986; Paige and Protopopescu, ISAJET) of jet physics, which are becoming better and better at building in realistic fragmentation and proper QCD evolution.

On the other hand, a wealth of experimental data now exists (Yamamoto, 1985; Sugano, 1986) reflecting different features of hard processes that now allow one to check very detailed predictions of the theory. These data, in particular, seem to indicate that the distribution of hadrons rather closely follows that of the fundamental partons of QCD, thus lending support to the idea of local parton-hadron duality (LPHD; Dokshitzer and Troyan, 1984; Azimov *et al.*, 1985a, 1987). In the LPHD approach, to be described in more detail in Sec. II, nonperturbative effects are reduced to normalizing constants relating hadronic amplitudes to partonic amplitudes.

Our object in this paper is to review briefly the physical origin of coherence effects in QCD (Ermolaev, and Fadin, 1984; Mueller, 1981; Bassetto *et al.*, 1982, 1983; Dokshitzer *et al.*, 1982a; Fadin, 1983) to summarize some of the striking experimental consequences of this coherence, and, especially, to suggest new ways in which this coherence may be seen in high-energy reactions.

In Sec. II, we shall review the basic ideas of coherence and discuss quantitative aspects using the modified leading logarithmic approximation (MLLA), an approximation that correctly keeps leading and next-to-leading logarithms (Mueller, 1983; Dokshitzer and Troyan, 1984) in jet evolution. The idea of angular ordering in jet evolution is explained in the context of a simple Abelian model. Moreover, in this simple model, the coherence that leads to the string or drag effect (Anderson *et al.*, 1983; Azimov *et al.*, 1985b, 1985c) in three-jet production is explained. We review briefly the difference predicted, and found (Aihara *et al.*, 1986; Sheldon *et al.*, 1986), in the hadrons associated with $q\bar{q}\gamma$ as compared to $q\bar{q}g$ events in e^+e^- annihilation. Analytic results are briefly summarized for the particle spectrum in jets, and we show how LPHD follows naturally at high energies.

In Sec. III we discuss experimental selection rules (Dokshitzer *et al.*, 1986). It is pointed out that forcing each hard-scattering event to correspond to a definite number of jets is probably not a good procedure. We em-

phasize the use of infrared stable criteria for jets and suggest that purely inclusive determinations of jet characteristics are probably the best way to make sharp connections between theory and experiment.

In Sec. IV a number of experiments are suggested in which the string effect may be visible in hadronic collisions (Dokshitzer *et al.*, 1986):

(i) In high-$p_\perp\gamma$ production, we point out that the Compton process $g+q\to\gamma+q$ can be isolated and a strong asymmetry of associated particles should be visible in the plane of the hard scattering.

(ii) In high-$p_\perp$ W production, different kinematic regions of the produced W favor either $q\bar{q}\to W+g$ or $gq\to Wq$, each of which as a distinctive asymmetry in the spectrum of associated particles. In kinematic regions where these two processes are comparable, it may be possible to tell, on an event-by-event basis, which subprocess has created the event by looking at the angular asymmetry of the associated hadrons.

(iii) In the production of two high-$p_\perp$ hadronic jets in $\bar{P}P$ collisions, certain kinematic regions make the subprocess $g+q\to g+q$ dominant. The associated asymmetry may allow one to distinguish the final gluon jet from that of the quark, at very high $p_\perp$'s, and so produce a sample of equal-energy quark and gluon jets. In each of the above cases estimates of the soft hadronic background are given.

In Sec. V, we discuss the hump-backed plateau (Dosshitzer *et al.*, 1982a; Mueller, 1983; Azimov *et al.*, 1986a), in the single-particle spectrum of QCD jets as a manifestation of coherence. We argue that it should be possible to see the movement of the peak of the single-particle spectrum as a function of jet energy, for jets produced in hadronic collisions, by considering only those particles lying within an angle $\theta_0/2$ of the jet axis. Explicit formulas are given.

In Sec. VI we briefly discuss the coherence of final-state hadrons produced in deeply inelastic lepton-hadron scattering. The situation here is richer than e^+e^- annihilation. There are two distinct jet regions. One of the jets, the jet struck by the virtual photon or W meson, has properties identical to those jets produced in e^+e^- annihilation or from high-$p_\perp$ hadron reactions. The other jet, the target jet, includes both hadrons from soft-hadron processes and hadrons originating from gluon emission from the parton lines evolving to the hard-scattering point. One again finds a hump in the distribution with the dip occurring for soft particles in a particular Breit frame described in Sec. VI.

II. THE ESSENCE OF COHERENCE IN HIGH-ENERGY REACTIONS

Our understanding of the structure of final hadronic states in hard processes has come a long way since the early eighties when the physics of coherence was rediscovered in the QCD context (Ermolaev and Fadin, 1981; Mueller, 1981; Bassetto *et al.*, 1982; Fadin, 1983).

First of all, the rapidly increasing wealth of experimental data makes it possible to test the adequacy of different phenomenological models of hadronization, a large variety of which had peacefully coexisted. Secondly, a number of well developed Monte Carlo schemes (Andersson *et al.*, 1983; Marchesini and Webber, 1984; Webber, 1984; Sjostrand, 1985, 1986; Field, 1986) have appeared, which incorporate the gross features of coherence in perturbative QCD. Finally, systematic perturbative techniques have been developed with which one can obtain reliable asymptotic expansions for many quantities describing multiparton systems.

A perhaps unexpectedly close correspondence between analytically described features of partonic systems and corresponding characteristics of measured final-state hadrons has led to the local parton-hadron duality hypothesis (LPHD; Azimov *et al.*, 1985a, 1987). The LPHD approach attempts to describe the general features of the hadronic systems produced in hard processes, such as multiplicity distributions, inclusive energy spectra and correlations, angular patterns of multiplicity and energy flow, etc., without invoking any hadronization scheme at all. This makes predictions very restrictive and, therefore, simply testable, since there are few parameters to vary in connecting perturbative QCD results to experiment. One of the main purposes of the LPHD approach is to look for phenomena where perturbation theory disagrees with experiment, in order to deduce some actual knowledge about the physics of confinement.

Before turning to specific analytical results in perturbative QCD, let us say a few words about the spirit of the perturbative approach to multiparticles systems and give a simple qualitative explanation of coherence.

Exact calculations of QCD matrix elements for multiparton systems are difficult to use even in the cases where they can be obtained. Thus the parton shower picture (Konishi *et al.*, 1979; Bassetto *et al.*, 1980, 1983; Dokshitzer *et al.*, 1982b; Dokshitzer and Troyan, 1984), in which one views the evolution, say, of a jet as a sequence of parton branchings, turns out to be a practical way to predict the properties of multiparton states. Generally speaking, using a shower picture does not necessarily lead to a loss of accuracy in describing multiparton phenomena. The main idea of the shower picture is to reorganize the perturbative expansion in such a way that its zero-order approximation is systematic and involves an arbitrary number of produced particles. This zero-order approximation can be achieved through an iteration of basic $A\to B+C$ parton branchings. In principle, it should be possible to include higher corrections to the basic branching along with higher point branching vertices $A\to B+C+D\ldots$ in order to improve the accuracy of a calculation systematically. This procedure (Dokshitzer and Troyan, 1984) is closely related to a renormalization-group approach (Mueller, 1983) in which the branchings are not so visible and in which high-order corrections can be systematically calculated.

The above-mentioned zero-order approximation is the

modified leading logarithmic approximation (MLLA; Dokshitzer and Troyan, 1984), which includes double logarithmic and single logarithmic effects in a systematic way (Mueller, 1983; Dokshitzer and Troyan, 1984). Of course this approximation has built in all the coherence effects in the quantum mechanics of gauge theories, since the approximation is systematic in α_S. Roughly speaking, there are two types of coherence effects that occur.

The first manifestation of coherence is the angular ordering of the sequential parton decays. This will be explained in more detail later on. Such angular orderings can be implemented in Monte Carlo simulations (Marchesini and Webber, 1984; Webber, 1984) of jet evolution, which are then able to reproduce this part of perturbative evolution correctly. Coherence of the second type (Azimov *et al.*, 1985b, 1985c, 1986a, 1986b) deals with the angular structure of particle flows when three or more partons are involved in a hard process. Here, single-jet evolution is no longer dominant and the particles produced in the regions between the jets depend on the geometry and color topology of the whole jet ensemble. The idea of an isolated jet evolution is here lost. It remains an open question to what extent this coherence can be generated in Monte Carlo simulations.

To elucidate the physical origin of angular ordering let us consider a simple model of the jet cascade, namely, the radiation pattern of soft photons produced by a relativistic e^+e^- pair in a QED shower (see Fig. 1). The question is to what extent the e^+ and e^- independently emit γ's. To answer this question one has to estimate the formation time, the time interval needed for the γ quantum to be radiated from , say, the p_e leg. Using the uncertainty relation to estimate the "lifetime" of the intermediate electron having virtual mass $M=\sqrt{(p+k)^2}$, one finds

$$t_{\text{form}} \approx \frac{1}{M}\frac{|\mathbf{p}_e|}{M} = \frac{p_e}{(p_e+k)^2} \approx \frac{1}{k\theta_{\gamma e}^2} ,$$

where $\theta_{\gamma e}$ is the angle between the emitted photon and the electron. Now $k\theta_{\gamma e}=k_\perp=\lambda_\perp^{-1}$ with $\lambda_\perp$ the transverse wavelength of the radiated photon. Thus

$$t_{\text{form}} \approx \lambda_\perp/\theta_{\gamma e} .$$

During this period of time the e^+e^- pair separate, transversely, a distance

$$\rho_\perp^{e^+e^-} \approx \theta_{e^+e^-} t_{\text{form}} \approx \lambda_\perp \frac{\theta_{e^+e^-}}{\theta_{\gamma e^-}} .$$

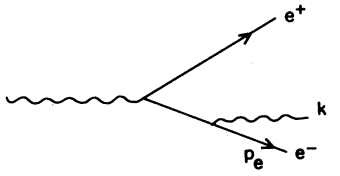

FIG. 1. Emission of soft photon k, after e^+e^- pair production.

One concludes that, for large-angle photon emissions,

$$\theta_{\gamma e^-} \approx \theta_{\gamma e^+} \gg \theta_{e^+e^-} ,$$

the separation of the two emitters e^+ and e^- is smaller than $\lambda_\perp$. In this case the emitted photon cannot resolve the internal structure of the e^+e^- pair and probes only its total electric charge, which is zero. Thus for $\theta_{\gamma e^-} \gg \theta_{e^+e^-}$ we expect photon emission to be strongly suppressed. This is the Chudakov effect, familiar in cosmic-ray physics (Chudakov, 1955). The e^+ and e^- can be said to emit photons independently only when $\rho_\perp^{e^+e^-} \gg \lambda_\perp$, that is, when $\theta_{\gamma e^+}, \theta_{\gamma e^-} < \theta_{e^+e^-}$.

The same discussion can be given for QCD cascades in which soft-gluon radiation is governed by the conserved (color) currents. The only difference is that the coherent radiation of soft gluons by an unresolved pair of gluons, or quarks, is no longer zero, but the radiation acts *as if* it were emitted from the parent gluon *imagined* to be on shell. This is illustrated in Fig. 2. The remarkable fact is that one gets all leading double and single logarithmic effects correctly, for angular averaged observables, by allowing the gluon emission, independently, off line 1 when $\theta_{1k} < \theta_{12}$, off line 2 when $\theta_{2k} < \theta_{12}$, and off the parent, line g, when $\theta_{kg} > \theta_{12}$ (see Fig. 2). This observation furnishes the core idea of the Marchesini-Webber model (Marchesini and Webber, 1984), the first Monte Carlo simulation that included coherence effects.

The best example of QCD coherence of the second kind is the string (or drag) effect observed in three-jet production in e^+e^- annihilation (Azimov *et al.*, 1985c; Andersson *et al.*, 1983). In Sec. IV, we shall have much more to say about this coherence; our purpose here is simply to explain the basic ideas. As yet, the most striking experimental test of this idea is the comparison of associated hadron production in $q\bar{q}g$ three-jet events with that of $q\bar{q}\gamma$ events with the g and γ having similar kinematics. In the plane of the three jets, counting the photon as a jet, one finds a suppression of associated hadrons in the region between the q and $\bar{q}$ in $q\bar{q}g$ events as compared to $q\bar{q}\gamma$ events. This effect was originally predicted in the Lund model (Andersson *et al.*, 1983) but is difficult to arrange in Monte Carlo branching models.

To illustrate the physical origin of the destructive interference one can use QED as a model, with the quark and antiquark replaced by e^-'s and the gluon by a collinear e^+e^+ pair as shown in Fig. 3. A simple calculation shows that there is no radiation emitted directly opposite the e^+e^+ pair in the symmetric configuration. In the QCD case, illustrated in Fig. 4, the associated soft-gluon radiation is

$$8\pi\frac{dN_g}{d\mathbf{n}}\alpha N_c\left[\frac{a_{23}}{a_2a_3}+\frac{a_{13}}{a_1a_3}\right]-\frac{1}{N_c}\frac{a_{12}}{a_1a_2} \quad (1)$$

in the $q\bar{q}g$ case and

$$8\pi\frac{dN_\gamma}{d\mathbf{n}}\alpha 2C_F\frac{a_{12}}{a_1a_2} \quad (2)$$

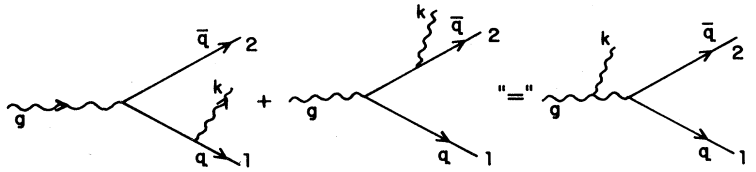

FIG. 2. An illustration of coherence in which wide-angle emission of soft gluon k, off q and $\bar{q}$, acts as if the emission came off the parent gluon g.

in the $q\bar{q}\gamma$ case, with the proportionality indicated in Eqs. (1) and (2) being an equality for inclusive gluon emission, without further cascading, from the hard-scattering graph of Fig. 4. In the above,

$$a_{ij}=1-\mathbf{n}_i\cdot\mathbf{n}_j\ ,$$
$$a_i=1-\mathbf{n}\cdot\mathbf{n}_i\ , \tag{3}$$

where $\mathbf{n}_i$ is the direction of jet i and $\mathbf{n}$ the direction of the additional, inclusive, soft gluon. For example, suppose $\mathbf{n}_1\mathbf{n}_2=\mathbf{n}_1\mathbf{n}_3=\mathbf{n}_2\mathbf{n}_3$ and $\mathbf{n}$ points in a direction exactly opposite to $\mathbf{n}_3$, that is, midway between the directions $\mathbf{n}_1$ and $\mathbf{n}_2$. Then

$$\frac{dN_g/d\mathbf{n}}{dN_\gamma/d\mathbf{n}}=\frac{N_c^2-2}{2(N_c^2-1)}=\frac{7}{16}\ . \tag{4}$$

It remains a challenge to Monte Carlo branching models to build in this result. In hadron production associated with the three-jet events $q\bar{q}g$ and $q\bar{q}\gamma$, Eq. (4) should remain correct, since hadronization effects should cancel, at least at high energies.

The observations of the above coherence phenomena (Bartel *et al.*, 1983; Aihara *et al.*, 1986; Hofmann, 1986; Sheldon *et al.*, 1986) can be said to test very detailed features of color flow in QCD. Later on, in Sec. IV, we shall discuss similar drag effects which manifest QCD coherence in hadronic collisions.

In the last part of this section we shall summarize briefly the more technical aspects of the hadronic composition of jets. There has been much technical progress in the past 5 or 6 years in understanding how to calculate particle spectra and correlations in QCD jets. Let us begin with the distribution, in x, of hadrons of type h in a gluon jet, $\bar{D}_g^h(x,Y)$. Then (Azimov *et al.*, 1985a, 1987)

$$x\bar{D}_g^h(x,Y)=\frac{4N_c}{bB(B+1)}Y \times\int_{a-i\infty}^{a+i\infty}\frac{d\omega}{2\pi i}x^{-\omega}K^h(\omega,M_h)\Phi(\omega,Y)\ , \tag{5}$$

where

$$\Phi=\Phi(-A+B+1,B+2;-\omega Y) \tag{6}$$

is the usual confluent hypergeometric function, with

$$A=\frac{4N_c}{b\omega},\quad B=\left[\frac{11N_c}{3}+\frac{2n_f}{3N_c^2}\right]\Big/b\ ,$$
$$b=\tfrac{11}{3}N_c-\tfrac{2}{3}n_f\ , \tag{7}$$

and

$$Y=\ln E/\Lambda\ . \tag{8}$$

In the above, E is the jet energy. In the case when the jet is restricted to have opening angle θ, Y should be replaced by

$$\ln\left[\frac{E\sin\frac{\theta}{2}}{\Lambda}\right].$$

Equation (5) is valid for particles not too far from the peak of the x distribution, and this equation, the modified leading logarithmic approximation (MLLA), includes all leading and next-to-leading logarithmic corrections. The jet energy dependence is contained in Φ, while fragmentation dependence is in K^h, which may depend on ω and on the QCD parameter Λ in a nonperturbative way. We indicate the dependence on nonperturbative QCD through the variable M_h, the mass of the hadron h.

When h is a gluon of mass Q_0, K^h is replaced, in per-

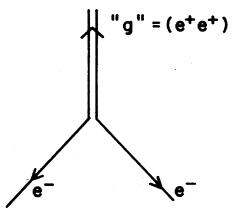

FIG. 3. Abelian model for illustrating string effect. The "gluon" is represented as having double the electric charge of the electron.

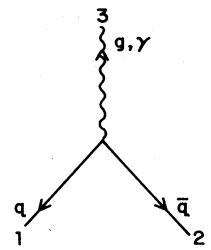

FIG. 4. QCD three-jet or two-jet emission with hard-photon processes.

turbation theory, by K^g, a purely perturbative quantity given by

$$K^g(\omega,\lambda)=\frac{\Gamma(A)}{\Gamma(B)}(\lambda\omega)^B\psi(A,B+1;\omega\lambda)\ , \tag{9}$$

with ψ the confluent hypergeometric function as defined in Erdelyi (1953) and $\lambda=\ln Q_0/\Lambda$. From Eqs. (5) and (9) it is clear that Φ includes evolution from scale E to scale Λ, while $K^g(\omega,\lambda)$ evolves the jet from Λ to Q_0. Thus

$$K^g(\omega,0)=1\ , \tag{10}$$

while $K^h(\omega,M_h)$ gives the transition of partons of scale Λ into hadrons of type h and mass M_h. Of course it is a phenomenological question at exactly what mass scale nonperturbative effects become important in the conversion of partons to hadrons. If the scale is μ, then K^h must include a perturbative evolution from Λ to μ and then a nonperturbative transition into hadrons. However, factorization, and the fact that perturbation theory itself gives color shielding (Bassetto *et al.*, 1983; Amati and Veneziano, 1979), lead one to conclude that μ should be Q independent. This, as we shall see below, leads to the idea of local parton-hadron duality (LPHD).

Consider now the large-Y limit of Eq. (5). It is straightforward to see that the dominant contribution, the saddle-point contribution, comes when $\omega\sim 1/\sqrt{Y}$. Since K^h is regular at $\omega=0$, one may simply let $K^h(\omega,M_h)\to K^h(0,M_h)=K^h$, since the ω dependence of $K^h(\omega,M_h)$ gives $\sqrt{\alpha}$ corrections to the MLLA approximation.

It is perhaps surprising to see the x dependence of $x\bar{D}_g^h$ being given completely in terms of parton evolution, with fragmentation contributing only a constant factor. Indeed, fragmentation effects have the possibility of smearing the hadron distribution over a finite interval in $\ln 1/x$; however, the smearing is formally a higher-order effect and need not be considered at the MLLA level. This is the statement of local parton-hadron duality (Azimov *et al.*, 1985a, 1987). Whether or not present jet energies are sufficiently large for LPHD to be applied is of course an experimental question. So far, the experimental evidence suggests that LPHD works rather well. A detailed discussion in given in Azimov *et al.* (1985a).

It is instructive to consider the situation in which h is a hadron consisting of a heavy quark and one or more light quarks. Here one would expect the momentum of the hadron to follow the momentum of the heavy quark more completely than in the case of light-hadron production. That is, fragmentation effects should be smaller in heavy-hadron production and LPHD should set in at lower jet energies. In fact, if one sums over all hadrons containing a particular heavy quark H, one should recover the distribution of the heavy quark H in the jet, $x\bar{D}_g^H$, which is calculable within perturbation theory, since one may follow the perturbative evolution all the way to the scale M_H without encountering strong nonperturbative effects. Thus the distribution of heavy hadrons in jets may be an especially useful measure of parton evolution.

III. ON EXPERIMENTAL SELECTION PROCEDURES

Traditionally (Dokshitzer *et al.*, 1986), the final-state structure in a hard collision is organized in terms of a certain number of jets having specific angles, energies, masses, etc. This has been a very fruitful procedure especially as regards three-jet events in e^+e^- collisions, where the gluon was found, and two-high-$p_\perp$-jet events in hadronic collisions, where the pointlike nature of quark and gluon interactions has been best measured. However, the separation of an event into a certain number of jets is inherently ambiguous, especially as one goes to higher energies. The ambiguity comes from several sources. (i) In a particular part of an event it may be equally correct to identify a set of particles as belonging to one jet, two jets, or even more jets. After all, a jet often has an identifiable substructure consisting of further jets. (ii) Some particles may not belong to any particular jet but may have emission properties dependent on a jet ensemble. The spectrum of particles associated with three-jet events in e^+e^- annihilation, especially in the wide-angle regimes, if of this character.

Attempting to force particles to belong to some jet in an event may cause difficulties. If the jet algorithms do not use infrared-safe quantities, comparison with QCD cannot be carried to higher orders, and the whole procedure, although adequate when only crude data and crude calculations are available, may have limited quantitative significance. If the jet-finding algorithms are infrared stable, the procedure for assigning particles to jets is in principle all right, but as higher-energy events become more complicated this procedure may simply not be efficient.

Especially as higher energies are attained it seems to us that a purely inclusive procedure for quantitatively dealing with hard collisions is preferable to organizing the event according to a certain number of jets. There is in general a rather direct correspondence between jets and energy correlations, so that any observable that can be described in terms of jets can also be described in terms of energy correlations (Basham *et al.*, 1978; Dokshitzer *et al.*, 1978). As an example consider the classic observation of the string effect as discussed in the previous section. Here one takes three-jet events in e^+e^- annihilation and projects the momenta of associated particles onto the plane determined by the three-jet axes. The suppression of particles between the q and q jets in qqg events is a direct measure of the coherence or of the amount of nonindependence in the different jet decays. This same physics is accessible through an (energy) multiplicity correlation (Dokshitzer and Troyan, 1984)

$$\sum\int dE_1E_2dE_2E_3dE_3E_4dE_4 \times\frac{d\sigma}{dE_1dE_2dE_3dE_4d\Omega_1d\Omega_2d\Omega_3d\Omega_4}\ ,$$

where the sum is over all particle types. The energy-weighted integrals over E_2,E_3,E_4 at fixed angular direc-

tions, specify the "jet" directions about which one has an associated multiplicity distribution at variable angular direction Ω_1. It should be possible to see the string effect in this observable in perhaps a more quantitatively significant way than has been done in the past.

In the sections that follow we shall refer to measurements involving determinations of jets and jet axes. To see, qualitatively, the effects we shall be considering, even crude determinations of jet axes are probably sufficient. However, in making precise quantitative relation to theory the use of energy and multiplicity correlations is preferable.

IV. DRAG EFFECTS IN HIGH-$p_\perp$ HADRONIC COLLISIONS

In this section we shall discuss the soft-gluon emission accompanying a high-$p_\perp$ hadronic collision. It is known that the background of soft particles accompanying a hard collision is significantly enhanced as compared to the spectrum in a minimum-bias event. The exact cause of this enhancement is unknown, as is the portion due to soft gluons emitted directly from the partons involved in the hard scattering. Our task here is to describe the size and angular distribution of such soft emissions in different types of hard scatterings and in particular to study the interference pattern that emerges when the soft gluons are emitted from several sources in a coherent manner. We begin our detailed description of these "drag" effects by considering hard processes where a high-$p_\perp\gamma$, W, or Z is produced along with a recoil parton. Later, we shall study the soft-gluon spectrum associated with two-jet production.

A. Prompt γ, W, Z production at large $p_\perp$

Prompt γ (or $W, Z \ldots$) production at collider energies furnishes a process similar to three-jet production in e^+e^- annihilation for studying interference (string) effects (Andersson *et al.*, 1982). The basic graphs describing the process are shown in Fig. 5. we shall argue in a moment that $gq \to \gamma q$ dominates $q\bar{q} \to \gamma g$. Keeping only the hard Compton scattering process, the cross section for producing a hard photon of transverse momentum $p_\perp = E$, corresponding to 90° scattering in the center-of-mass system of the parton-parton scattering, is (Eichten *et al.*, 1984)

$$\frac{d\sigma}{dp_\perp^2 d\cos\theta} = \sum_q e_q^2 \int dy\, x_q D_P^q(x_q, p_\perp^2) x_g D_{\bar{P}}^g(x_g, p_\perp^2) \frac{d\sigma}{dp_\perp^2} + (P \leftrightarrow \bar{P}) , \tag{11}$$

with D_P^q the quark distribution of the proton P. (We use the notation D for structure functions and $\bar{D}$ for fragmentation functions.) In the above, $x_g x_q s = 4p_\perp^2$ and $y = y_1 + y_2$, with y_1 and y_2 the *rapidities* of the outgoing γ and gluon jets, respectively. As usual e_q is the electric charge of the quark having flavor q. Then

$$\frac{d\sigma}{dp_\perp^2 dy\, d\cos\theta} = \sum_q e_q^2 \frac{5\pi\alpha_{\rm EM}\alpha}{96 p_\perp^4} x_q D_P^q(x_q, p_\perp^2) x_g D_{\bar{P}}^g(x_g, p_\perp^2) + (P \leftrightarrow \bar{P}) . \tag{12}$$

The corresponding formula for the hard process $q\bar{q} \to \gamma g$ is

$$\frac{d\sigma}{dp_\perp^2 dy\, d\cos\theta} = \sum_q e_q^2 \frac{\pi\alpha_{\rm EM}\alpha}{9 p_\perp^4} x_q D_P^q(x_g, p_\perp^2) x_{\bar{q}} D_{\bar{P}}^{\bar{q}}(x_{\bar{q}}, p_\perp^2) + (P \leftrightarrow \bar{P}) . \tag{13}$$

When $x_{\bar{q}}(x_g)$ is less than about 0.1, the Compton process dominates over annihilation, and so we shall neglect the contribution given by Eq. (13).

Now to the main point of this section. In addition to the jet produced in the hard collision there are also soft-gluon emissions associated with the incoming quark and gluon lines and with the final-state quark which lead to an interference pattern (drag effect) almost exactly as in the process $e^+e^- \to g\bar{q}q$ + soft gluons. The picture of the soft-gluon emissions is schematically illustrated in Fig. 6. [The QCD description (Dokshitzer *et al.*, 1986) of the process is qualitatively similar, in terms of color topology, to the Lund description (Andersson *et al.*, 1982).] The formula for soft-gluon emission, in direction **n**, asso-

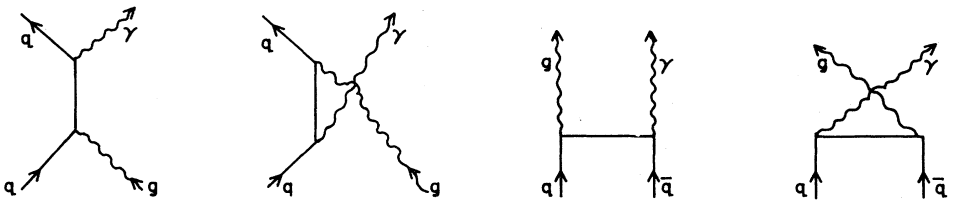

FIG. 5. Hard-scattering graphs leading to γ + jet production.

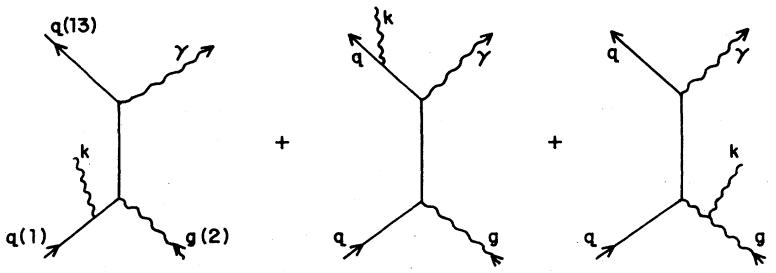

FIG. 6. Soft-gluon emission from the hard-scattering graphs of Fig. 5.

ciated with the hard scattering is

$$8\pi\frac{dN}{d\mathbf{n}}=\left[\left[\frac{a_{23}}{a_2a_3}+\frac{a_{12}}{a_1a_2}\right]-\frac{1}{N_c^2}\frac{a_{13}}{a_1a_3}\right]N_g'(Y) \tag{14}$$

with

$$\begin{aligned} a_{ij}&=1-\mathbf{n}_i\mathbf{n}_j\ , \\ a_j&=1-\mathbf{n}\mathbf{n}_i\ , \end{aligned} \tag{15}$$

where $\mathbf{n}_i$ is the direction of the parton $i=(1)$–(3) as shown in Fig. 7, and $N_g'(y)$ is the derivative of N_g with respect to Y. The factor $N_g'(Y)$ (Azimov *et al.*, 1985a, 1986b; Dokshitzer *et al.*, 1986) takes into account that the final "measured" gluon is part of a cascade. The variable $Y=\ln E\theta/\Lambda$ is the logarithmic variable governing the evolution of a jet of momentum E and opening angle θ. In the above, $\theta=\min\{\theta_1,\theta_2,\theta_3\}$ with $\cos\theta_i=\mathbf{n}\cdot\mathbf{n}_i$. Equation (14) gives the parton evolution correctly through leading and next-to-leading terms, the modified leading logarithmic approximation. In this approximation we may write N_g as (Azimov *et al.*, 1985a, 1987)

$$N_g(Y)=x_1\left[\frac{x_2}{x_1}\right]^B[I_{B+1}(x_1)K_B(x_2)+I_B(x_2)K_{B+1}(x_1)]\ , \tag{16}$$

with I and K modified Bessel functions and with

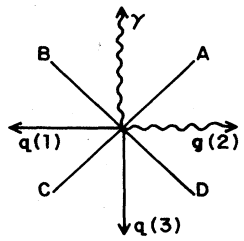

FIG. 7. The kinematics of 90° scattering in the hard process for γ+jet production.

$$x_1=\left[\frac{16N_c}{b}Y\right]^{1/2},\quad x_2=\left[\frac{16N_c}{b}\ln Q_0/\Lambda\right]^{1/2},$$

where

$$B=\left[\frac{11N_c}{3}+\frac{2n_f}{3N_c^2}\right]\Big/b\ .$$

Here $b=11/3N_c-2/3n_f$ and Q_0 is the cutoff on soft-gluon emissions. When x_1 is large and $x_1/x_2\gg1$ one has

$$N_g(Y)\sim x_2^BK_B(x_2)x_1^{-B+1/2}\frac{e^{x_1}}{\sqrt{2\pi}}\ . \tag{17}$$

As discussed earlier, a reasonable phenomenology can be done for $\pi^\pm$ production taking $N_g^\pi=K^\pi N_g$ where one also takes $Q_0=\Lambda$, in which case

$$N_g^\pi\sim K^\pi\left[\frac{x_1}{2}\right]^{-B+1/2}\frac{\Gamma(B)}{2\sqrt{\pi}}e^{x_1}\ . \tag{18}$$

In Azimov *et al.* (1985a, 1987), $K^\pi=1.1$ for charged pions was obtained using Eq. (16) with $Q_0=\Lambda$. This determination corresponds to a total charged-pion multiplicity of about 11 in an e^+e^- annihilation event at $Q\approx30$ GeV. The expected multiplicity in a gluon jet should be about the same. Because it is easier to illustrate our discussion here, we shall use Eq. (18) rather than (16), in which case $K^\pi\approx0.6$ is more appropriate. The difference between Eqs. (16) and (18) is a series of terms of inverse powers of $\sqrt{Y}$, terms which have not systematically been included in jet evolution so far. Since $\sqrt{Y}$ varies slowly, we do not expect important differences in predictions in the intermediate-energy region with which we are concerned.

Of course the coherence pattern for heavier particles, like K's or P's, can also be obtained from Eq. (16) in a manner that has already been discussed in Sec. II. We shall restrict our estimates here, however, to pions that furnish the bulk of the produced particles.

To see the structure of the coherence pattern we shall evaluate Eq. (14) for final-state pions in the plane of the hard scattering and at angles midway between the partons involved in the hard scattering, directions labeled by A, B, C, and D in Fig. 7. Thus $dN^A/d\mathbf{n}$ corresponds to the number density of pions in the plane of the hard

scattering and midway between the directions determined by the incoming gluon and the outgoing photon. [Note in Fig. 7 that $q(1)$ and $g(2)$ are incoming, while γ and $q(3)$ are outgoing lines.] For purposes of illustration we take $E=p_\perp=20$ GeV, at which value

$$N_g^\pi(Y)\approx 20K^\pi\Gamma(\tfrac{101}{81}) \tag{19}$$

and

$$\frac{d}{dY}N_g^\pi(Y)\approx 9K^\pi\Gamma(\tfrac{101}{81})\ . \tag{20}$$

Taking $K^\pi\Gamma(\frac{101}{81})=0.6$ we find

$$\pi\frac{dN^A}{d\mathbf{n}}\approx 4\ , \tag{21a}$$

$$\pi\frac{dN^B}{d\mathbf{n}}\approx 3\ , \tag{21b}$$

$$\pi\frac{dN^C}{d\mathbf{n}}\approx 3\ , \tag{21c}$$

$$\pi\frac{dN^D}{d\mathbf{n}}\approx 11\ . \tag{21d}$$

Two important questions remain to be answered before we are able to conclude that the drag effect described in Eq. (21) can be seen in a hadronic collision: (i) We need to estimate the hadronic background from other soft processes to see whether those pions coming from soft-gluon emission will be observable above that background. (ii) We need to estimate the size of the cross section given by Eq. (12) to see what transverse momenta are available for hard-photon production.

(i) For soft pions coming from the minimum-bias background we write

$$\frac{dN}{d\mathbf{n}}=\frac{1}{2\pi}\frac{dN}{d\cos\theta}=\frac{1}{2\pi}\frac{1}{1-\cos^2\theta}\frac{dN^{\rm soft}}{dy}\ , \tag{22}$$

with θ the angle of the pion with respect to the beam direction. We have evaluated Eq. (21) at $\theta=45°$ or 135°, which gives

$$\pi\frac{dN}{d\mathbf{n}}=\frac{dN^{\rm soft}}{dy}\ . \tag{23}$$

We expect that $dN^{\rm soft}/dy$ is certainly no greater than about 6 for charged pions, in which case the rate of pions given by soft-gluon emission from the hard-scattered partons, Eq. (21), should be dominant as far as the angular asymmetries in $dN/d\mathbf{n}$ are concerned.

(ii) To estimate the cross section for hard-γ production, we integrate Eq. (12) over $p_\perp^2>\bar p_\perp^{\,2}$, and take dy and $d\cos\theta$ intervals of one unit each. This leads to a hard-γ cross section

$$\sigma_\gamma=2\sum_q e_q^2\frac{5\pi\alpha_{\rm EM}\alpha}{96\bar p_\perp^{\,2}}x_qD_{\bar P}^q(x_q,\bar p_\perp^{\,2})x_gD_{\bar P}^g(x_g,\bar p_\perp^{\,2}) \tag{24}$$

or

$$\sigma_\gamma\approx\frac{2\times10^{-4}}{\bar p_\perp^{\,2}}x_qD_{\bar P}^ux_qD_{\bar P}^g\ . \tag{25}$$

For $\bar p_\perp=20$ GeV this leads to a hard-γ cross section per unit rapidity as

$$\sigma_\gamma\approx 2\times10^{-34}\ {\rm cm}^2x_qD_{\bar P}^ux_qD_{\bar P}^g\ , \tag{26}$$

which is probably large enough to allow measurement of such hard γ's at Fermilab. Of course, one can lower $\bar p_\perp$ somewhat to increase the cross section, but the coherence effect is dominated by hadronic background for $p_\perp<10$ GeV.

A process very similar to hard-γ production is that of high-$p_\perp$ W production. Here the production cross section is (Eichten *et al.*, 1984)

$$\frac{d\sigma}{dy_1dy_2dp_\perp^2}=\sum_{ij}x_1D_P^i(x_1,p_\perp^2)x_2D_{\bar P}^j(x_2,p_\perp^2)\frac{d\hat\sigma_{ij}}{dt}\ , \tag{27}$$

with i,j a sum over partons and $d\hat\sigma_{ij}/d\hat t$ the hard-scattering cross section $i+j\to W+$parton. y_1 and y_2 are the rapidities of the W and the recoil parton, while $p_\perp$ is the transverse momentum of the W. There are two fundamental hard processes: (i) $q+\bar q\to W+g$ and (ii) $q+g\to q+W$ or $\bar q+g\to\bar q+W$. The basic cross sections are

$$\text{(i)}\quad\frac{d\hat\sigma_{u\bar d}}{d\hat t}=\frac{2\pi\alpha_{\rm EM}\alpha}{9\sin^2\theta_W}\frac{(\hat t-M_W^2)^2+(\hat u-M_W^2)^2}{\hat s^{\,2}\hat t\,\hat u} \tag{28}$$

and

$$\text{(ii)}\quad\frac{d\hat\sigma_{ug}}{d\hat t}=\frac{\pi\alpha_{\rm EM}\alpha}{12\sin^2\theta_W}\frac{\hat s^{\,2}+\hat u^{\,2}+2M_W\hat t}{-\hat s^{\,3}\hat u}+(\hat t\leftrightarrow\hat u)\ . \tag{29}$$

Suppose we consider 90° scattering in the parton center-of-mass system. Then $\hat t=\hat u$. Further, when $p_\perp/M_W\ll1$, $\hat s\approx M_W^2+2p_\perp M_W$ while $\hat t$ and $\hat u$ equal $-p_\perp M_W$. Thus the ratio of Eq. (18) to Eq. (19) is $8M_W/3p_\perp$. When the parton distributions are included, the ratio of $q\bar q\to W$ + parton to $q(\bar q)+g\to q(\bar q)+W$ becomes

$$r=\frac{8M_W}{3p_\perp}\frac{D_P^u(x_1)D_{\bar P}^{\bar d}(x_2)+D_P^{\bar d}(x_1)D_{\bar P}^u(x_2)}{D_P^u(x_1)D_{\bar P}^g(x_2)+D_P^g(x_1)D_{\bar P}^u(x_2)}\ . \tag{30}$$

The size of r depends on $p_\perp$ and energy quite strongly. At CERN collider energies, where valence quark contributions are still dominant, r is larger than unity. At Fermilab collider energies, sea quark and gluon distributions become more important and $r\le1$, depending exactly on the region of x_1 and x_2 and on the values of $p_\perp$.

The associated soft-gluon spectrum is quite different in the Compton and annihilation processes. For $gq\to Wq$ the associated gluon spectrum is exactly as given by Eq. (14), while for $q\bar q\to w+g$ the associated gluon distribution is given by

$$8\pi\frac{dN}{d\mathbf{n}}=\left[\left[\frac{a_{13}}{a_1a_3}+\frac{a_{23}}{a_2a_3}\right]-\frac{1}{N_c^2}\frac{a_{12}}{a_1a_2}\right]N_g'(Y)\ , \tag{31}$$

where the lines are labeled as in Fig. 8 and the definition of a_{ij} and a_i is as before. Carrying out an analogous calculation to the one that led to Eq. (21) we now arrive at

$$\pi\frac{dN^A}{d\mathbf{n}}=\pi\frac{dN^B}{d\mathbf{n}}=1\ , \tag{32a}$$

$$\pi\frac{dN^C}{d\mathbf{n}}=\pi\frac{dN^D}{d\mathbf{n}}=8\ , \tag{32b}$$

where we have again taken $p_\perp=E=20$ GeV and have made use of Eq. (20). The distributions given by Eq. (21) and (32) are sufficiently different that the associated hadron distribution might make it possible to decide which production mechanism was responsible *for a given event.* In any case, as one varies energy and/or the x value and $p_\perp$ region considered, one favors either the Compton or annihilation process, and the associated hadron spectrum should follow Eq. (21) or (32) more closely depending on the exact kinematic region.

B. Two-jet production at high $p_\perp$

Coherence effects are more difficult to observe in the spectrum of hadrons associated with two-jet production than in γ or W production. Nevertheless, there are some specific effects that may be observable. The only hard-scattering process that has a large asymmetry in the spectrum of associated hadrons is $gq(\bar{q})\to gq(\bar{q})$, for which subprocess the two-jet cross section is

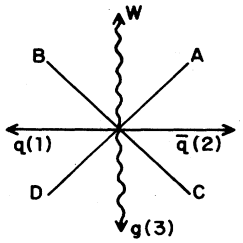

FIG. 8. The kinematics of 90° scattering in the hard process for W+jet production.

$$\frac{d\sigma}{dy_1dy_2dp_\perp^2}=x_qD_P^g(x_q,p_\perp^2)x_gD_{\bar{P}}^g(x_g,p_\perp^2)\frac{d\hat{\sigma}}{dp_\perp^2}+(P\leftrightarrow\bar{P})\ , \tag{33}$$

with $d\hat{\sigma}/dp_\perp^2$ referring to the fundamental hard process. In general, the process $gq\to gq$ does not dominate the competing hard processes such as $gg\to gg$, $q\bar{q}\to q\bar{q}$, etc. For jets having $p_\perp=90$ GeV at Fermilab, and with $x_g\approx0.03$ and $x_q\approx0.33$, the $gq\to gq$ part of the two-jet cross section is about 50% and rises very slowly as x_q further increases. Thus the sample of gq scatterings is in general contaminated by competing processes which have no asymmetry. We shall shortly return to the question of whether this signal may be observable.

The spectrum of hadrons associated with the hard process equation (33) is

$$\begin{aligned}8\pi\frac{dN}{d\mathbf{n}}=[H^c(\hat{t},\hat{u},\hat{s})]^{-1}\frac{2}{N_c}\Bigg[&H^c(\hat{t},\hat{u},\hat{s})\left[C_F\frac{a_{24}}{a_2a_4}+N_c\frac{a_{13}}{a_1a_3}\right]\\&-C_F\left[2\frac{a_{24}}{a_2a_4}+2\frac{a_{13}}{a_1a_3}-\frac{a_{23}}{a_2a_3}-\frac{a_{12}}{a_1a_2}-\frac{a_{34}}{a_3a_4}-\frac{a_{14}}{a_1a_4}\right]H_1^c(\hat{t},\hat{u},\hat{s})\\&+C_F\left[\frac{a_{12}}{a_1a_2}+\frac{a_{34}}{a_3a_4}-\frac{a_{23}}{a_2a_3}-\frac{a_{14}}{a_1a_4}\right]H_2^c(\hat{t},\hat{u},\hat{s})\Bigg]N_g'(Y)\ ,\end{aligned} \tag{34}$$

where we use the notation of Ellis *et al.* (1986) for the hard-scattering amplitudes, in which

$$H^c(s,t,u)=g^4C_F(t^2+u^2)\left[\left[1-\frac{1}{N^2}\right]\frac{1}{tu}-\frac{2}{s^2}\right],\quad H_1^c(s,t,u)=g^4\frac{N}{4}(t^2+u^2)\left[\left[1-\frac{2}{N^2}\right]\frac{1}{tu}-\frac{2}{s^2}\right],$$

$$H_2^c(s,t,u)=g^4\frac{N}{4}(t^2-u^2)\left[\frac{1}{tu}-\frac{2}{s^2}\right].$$

The incoming gluon and quark lines are labeled by 1 and 2, while the outgoing gluon and quark lines are labeled by 3 and 4 as shown in Fig. 9. For $\hat{t}=\hat{u}=-\hat{s}/2$, 90° scattering in the partonic center-of-mass system, one finds

$$\begin{aligned}\frac{8\pi\,dN}{d\mathbf{n}}=\frac{2}{N_c}\Bigg[&C_F\frac{a_{24}}{a_2a_4}+N_c\frac{a_{13}}{a_1a_3}-\frac{387}{704}C_F\left[2\frac{a_{24}}{a_2a_4}+2\frac{a_{13}}{a_1a_3}-\frac{a_{23}}{a_2a_3}-\frac{a_{12}}{a_1a_2}-\frac{a_{34}}{a_3a_4}-\frac{a_{14}}{a_1a_4}\right]\\&-\frac{243}{704}C_F\left[\frac{a_{12}}{a_1a_2}+\frac{a_{34}}{a_3a_4}-\frac{a_{23}}{a_2a_3}-\frac{a_{14}}{a_1a_4}\right]\Bigg]N_g'(Y)\ .\end{aligned} \tag{35}$$

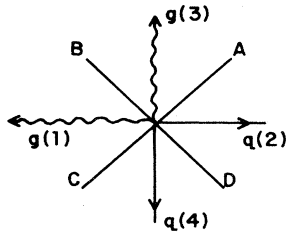

FIG. 9. The kinematics of 90° scattering in the hard process $q(2)+g(1)\rightarrow q(4)+g(3)$.

Evaluating Eq. (35) in the plane of the scattering and midway between the directions of the parton momenta, in the partonic center-of-mass frame, one finds

$$\pi\frac{dN^A}{d\mathbf{n}}=\pi\frac{dN^c}{d\mathbf{n}}\approx 1.7N_g'(Y)\ , \tag{36a}$$

$$\pi\frac{dN^B}{d\mathbf{n}}\approx 2.1N_g'(Y)\ , \tag{36b}$$

$$\pi\frac{dN^D}{d\mathbf{n}}\approx 0.5N_g'(Y)\ . \tag{36c}$$

For pion production, $d/dy\ N_g^\pi$ can be estimated from Eq. (18) to be $d/dy\ N_g^\pi\approx 9$ at $p_\perp=E=90$ GeV. Thus the asymmetry indicated in Eq. (36) should be observable above the normal soft hadronic background. However, the situation is quite different from the case of hard-γ or W production. There one had only a single outgoing jet. In the present situation there are two outgoing jets, and it is not apparent which one is the gluon and which one is the quark jet. Indeed, it is not even apparent whether the hard scattering has been a $gq\rightarrow gq$ event. One must, in fact, use the resulting asymmetry to try and distinguish $gq\rightarrow gq$ events from the other hard scatterings which are either exactly symmetric or very nearly symmetric, depending on the process. This is probably easiest in the kinematic regions having the largest rapidities, where the competing process is mainly $q\bar{q}\rightarrow q\bar{q}$, a process that has *weak* almost symmetric radiation and should look significantly different from $gq\rightarrow gq$ hard scatterings on an event-by-event basis.

Of course all of our calculations are for average properties. We have little to say about event-to-event fluctuations that depend on higher correlations. Fluctuations are probably best estimated by using Monte Carlo simulations; such simulations might be able to suggest more detailed tests for separating $gq\rightarrow gq$ scatterings from the competing processes and thus allow one to obtain a sample of separated high-$p_\perp$ quark and gluon jets in the same event. In any case, one will certainly wish to make use of the whole event structure and not just the differential asymmetries that we have calculated in Eq. (36).

V. FINDING THE HUMP-BACKED DISTRIBUTION

The depletion of small-x particles inside a jet, the so-called hump-backed plateau in the inclusive energy spectrum, remains one of the most striking predictions of perturbative QCD. The depletion of small-x particles follows from the angular ordering of partonic cascades in going from greater to lesser virtuality and is a direct manifestation of coherence in QCD. At present there is experimental evidence for such a nonflat plateau in e^+e^- annihilation, but the effect is less than definitive. It is one of the purposes of this section to suggest a way in which this distribution may more easily be found, especially in the very-high-energy jets available at hadronic colliders. Before coming to that point, though, we would first like to discuss some general questions related to the spectrum of particles in a jet (Azimov *et al.*, 1986a).

In discussing the spectrum of particles having small transverse momentum in hadronic collisions, the rapidity

$$y_{11}=\frac{1}{2}\ln\frac{E+p_\parallel}{E-p_\parallel} \tag{37}$$

has proved a useful variable. In Eq. (37), $p_\parallel$ is the component of momentum, of an outgoing particle, measured along the common direction determined by the incident hadrons. In jet production it is perhaps tempting to use a similar variable, where now $p_\parallel$ would be measured along the jet axis. However, for purposes of comparing QCD with jet measurements, $y_\parallel$ is not a good variable. The difficulty with $y_\parallel$ is

$$y_\parallel=-\ln\tan\theta/2 \tag{38}$$

for massless particles, and all particles within a subjet of a given jet have similar values of θ. Thus $y_\parallel$ gives essentially no information on the magnitude of the momentum of the measured particle in contrast to the situation in soft-hadron production where $y_\parallel$ is a quite good indicator of a particle's momentum.

In terms of $y_\parallel$ the coherence of QCD does not produce a dip in particle spectrum (Azimov *et al.*, 1986a). To see this in more detail, let $N(Y)$ be the number of particles within an angle θ of the jet axis of a jet having energy E. $Y=\ln E\theta/\Lambda$. Then, using

$$N(Y)=CY^{1/4-B/2}\exp\left[\left[\frac{16N_c}{b}Y\right]^{1/2}\right]\ , \tag{39}$$

one finds

$$\frac{dN}{dy_\parallel}=\frac{1}{2}\frac{16N_c}{\left[b\ln\left[\frac{E}{\Lambda c h y_\parallel}\right]\right]^{1/2}}N\ , \tag{40}$$

where we have used a small-angle approximation in obtaining Eq. (40). [At very small values of $y_\parallel$ the small-angle approximation is of course not good, but the level of accuracy of MLLA does not really allow a distinction between different ways of writing a large-angle generalization of Eq. (40).] Note that there is no hint of a dip in

Eq. (40) as $y_{\parallel}$ decreases.

What, then, is a good variable for describing the particle spectrum inside a jet? Either $x=p/E$ or $y=\ln(E_p+p)/m$ is fine. (E is the jet energy. p, E_p, and m are the momentum, energy, and mass of the measured particle.) For zero-mass particles, or at high momentum, $\ln 1/x$ and y differ by a constant and so are completely equivalent variables. Another virtue of x, or y, is that one does not need to know the jet axis accurately. In using $y_{\parallel}$ one may produce a dip at $y_{\parallel}=0$ simply from a bias against choosing the jet axis so that $y_{\parallel}=0$ (Azimov *et al.*, 1986a).

From Eq. (5), we may find the asymptotic shape of the single-particle distribution as

$$x\bar{D}(x,Y)=N(Y)\left[\frac{36N_c}{\pi^2 bY^3}\right]^{1/4}\exp\left[-\left[\frac{36N_c}{b}\right]^{1/2}\frac{\left[\ln\frac{1}{x}-\frac{1}{2}Y-B\left[\frac{b}{16N_c}Y\right]^{1/2}\right]^2}{Y^{3/2}}\right] \tag{41}$$

not too far from the peak of the distribution. For purposes of our present discussion the main point is that the distribution should reach its maximum at

$$\ln\frac{1}{x_0}=\frac{1}{2}Y+B\left[\frac{b}{16N_c}Y\right]^{1/2} \tag{42}$$

and have a broad Gaussian shape about that peak. It is the decrease of $x\bar{D}(x,Y)$ for values of $x<x_0$ which is the dip in the single-particle spectrum caused by coherent radiation in QCD.

Unfortunately, the momentum corresponding to the x_0 in Eq. (42) is not large at present energies. Indeed, this momentum grows rather slowly with the jet energy. Furthermore, phase space requires that $x\bar{D}(x,Y)$ have a zero at the kinematic minimum value of x, and it is very difficult to disentangle the kinematic dip in the spectrum from the dynamical dip required by Eq. (41). So far, probably the most convincing evidence for the hump-backed distribution is the growth of the energy, $E_{\text{hump}}=E_0=x_0E$, at which the distribution reaches its maximum as one varies the jet energy (Althoff *et al.*, 1984). Additional data for higher-energy jets at SLAC Linear Collider (SLC) should make this growth much clearer and perhaps allow one to check the relation

$$\frac{E}{E_0}\frac{dE_0}{dE}=\frac{1}{2}-B\left[\frac{b}{64N_cY}\right]^{1/2}. \tag{43}$$

Equation (43) gives

$$\frac{d\ln(E_0/\Lambda)}{d\ln(E/\Lambda)}\approx 0.4 \quad \text{at } E\approx 30 \text{ GeV}.$$

To sharpen the influence of angular ordering on the parton multiplication process, and in an attempt to find the dip in the soft part of the spectrum in jets produced in hadronic collisions, it may be useful to look at particles restricted to lie within a particular opening angle with respect to the jet. For example, we might consider the y distribution of particles accompanying the production of an energetic particle and lying within an opening angle θ_0 about the direction of the trigger particle momentum. Or, in the spirit of our discussion in Sec. III, one could look at the two-particle inclusive correlation between energy and particle flows,

$$x_1\frac{d\sigma}{dx_1}=\int_{\cos\theta_0}^{1}d\cos\theta_{12}\int_0^1 dx_2 x_1 x_2\frac{d\sigma}{dx_1dx_2d\cos\theta_{12}}. \tag{44}$$

As is easily seen, parton cascades in these situations will populate mainly the region

$$\frac{Q_0}{\sin\theta_0/2}<E_1<E, \tag{45}$$

with $E_1=x_1E$, the momentum of the observed particle, E the jet energy, and Q_0 the cutoff point on the evolution. $Q_0\approx m_1$, the mass of the observed particle.

The maximum of the distribution, in E_1, is now forced to larger energies as compared to Eq. (42). The maximum of the distribution now occurs at

$$\ln\frac{E_1}{Q_0}=\frac{1}{2}\ln\frac{E}{Q_0\sin\theta_0/2}-B\left[\frac{b}{16N_c}\right]^{1/2}\left[\left[\ln\frac{E\sin\theta_0/2}{\Lambda}\right]^{1/2}-\left[\ln\frac{Q_0}{\Lambda}\right]^{1/2}\right], \tag{46}$$

which formula replaces Eq. (42). Clearly, by choosing θ_0 small one can move the peak of the distribution away from phase-space limit of $E_1\approx Q_0$. There are, however, some subtleties connected with the use of restricted angular regions to find the hump-backed distribution.

(i) Decreasing θ_0 to stiffen the spectrum inevitably results in a decrease of the overall height of the peak of the distribution, since the predicted spectrum should look like an "unrestricted" particle distribution inside a jet with smaller effective energy, $E^{\text{eff}}\approx E\sin\theta_0/2$, boosted along the jet direction by an amount $\Delta y\approx -\ln(\sin\theta_0/2)$. However, by choosing an appropriate value of θ_0 one may retain a large enough peak while removing the

domain of nonrelativistic momenta.

(ii) Perhaps a more serious problem is that a distribution that has no dip at small values of x may acquire such a dip because of the angular cut, θ_0. For example, if one were to solve the evolution equation for the single-particle spectrum using only ladder graphs *without imposing angular ordering* one would find

$$x_1 D(x_1, Y) \alpha \exp\left[\frac{2\alpha N_c}{\pi}\left[\ln\frac{E\sin\theta_0/2}{Q_0} - \tfrac{1}{2}\ln 1/x_1\right]\ln 1/x_1\right]^{1/2} . \quad (47)$$

[Equation (47) comes from a leading double logarithmic calculation at fixed coupling and is given for illustrative purposes only.] The maximum of this distribution occurs at

$$\ln\frac{E_1}{Q_0} = -\ln(\sin\theta_0/2) , \quad (48)$$

which expression should be compared with Eq. (46). For θ_0 large the distribution has no dip in the region $E_1/Q_0 \gg 1$. However, the angular constraint θ_0 creates a hump-backed plateau here, also. Thus one cannot simply use the existence of a hump-backed distribution, when θ_0 is small, to measure perturbative coherence. Nevertheless, if one chooses θ_0 moderately small and varies the jet energy, coherence will give a moving peak, while the peak determined at Eq. (48) is jet-energy independent. Thus, taking the derivative of Eq. (46) with respect to E,

$$\frac{E}{E_1}\frac{dE_1}{dE} = \frac{1}{2} - B\left[\frac{b}{64 N_c Y(\theta_0)}\right]^{1/2} , \quad (49)$$

with

$$Y(\theta_0) = \ln\frac{E\sin\theta_0/2}{\Lambda} .$$

This equation is almost identical to Eq. (43), but in hadronic reactions one has the possibility of measuring larger jet energies and so better determining the slope given by Eq. (49).

Attempting to see the hump-backed distribution in jets produced in hadronic collisions it is necessary to control the background due to the soft hadrons present in any hadronic collision. The angular cut θ_0 described above is especially useful in this respect, since one is able to eliminate much of the soft background simply by reducing the phase space available to the soft particles. We have calculated the expected charged-particle distribution for jets of 50 GeV, energies accessible at SLC and LEP, and 150 GeV, appropriate for the Fermilab collider and for θ_0 values between 10° and 60°. The number of hadrons in either quark or gluon jets can be obtained from $x\bar{D}_g^g(x, Y, \lambda)$ [see Eqs. (5) and (9)] at least as far as the small-x part of the spectrum is concerned. To get the

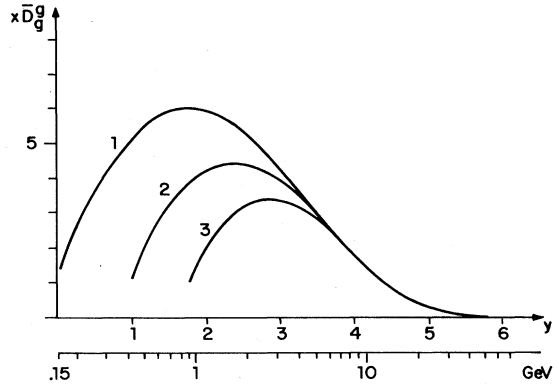

FIG. 10. Energy distribution of charged hadrons (vs $y = \ln E_h/\Lambda$) in different cones around the jet axis in e^+e^- annihilation at $W_{e^+e^-} = 100$ GeV: (1) for the whole opening angle $\theta = 180°$; (2) $\theta = 45°$; (3) $\theta = 20°$. Numerically, these spectra coincide with appropriate parton spectra $x\bar{D}_g^g$ for the so-called "isolated" g jet.

charged-hadron spectrum for a gluon jet one multiplies $x\bar{D}_g^g$ by a factor ≈ 1.1 and sets $Q_0 \approx \Lambda \approx m_\pi$. (In analyzing data from e^+e^- collisions, one must also take into account the influence of heavy-quark jets on the spectrum.) For hadrons contained in a single quark jet a factor $\frac{4}{9}$ must be included. When θ_0 well contains the jet, but is sufficiently small to avoid the coherent influence of other jets, and E is large, we may expect the famous $\frac{9}{4}$ factor to describe accurately the difference between quark and gluon jets.

In Figs. 10 and 11, the expected distributions are shown for charged hadrons along with a rough estimate of the background obtained by assuming a soft-hadron component of $dN^{\text{charged}}/dy = 6$ uniformly distributed in

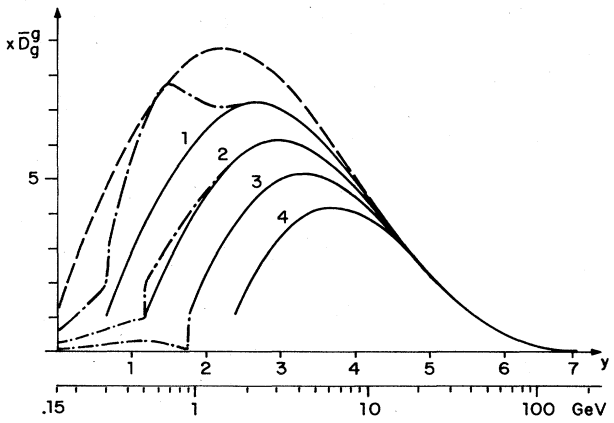

FIG. 11. Energy spectra of partons ($y = \ln E_p/\Lambda$) in g jet produced in high-$P_\perp$ process at $P_\perp$ (or $E_\perp$) ≈ 150 GeV in different cones around the jet axis: (1) $\theta = 60°$; (2) $\theta = 35°$; (3) $\theta = 20°$; (4) $\theta = 10°$. The dashed curve shows the total spectrum of the nonavailable "isolated" g jet. A typical change of spectra due to background is shown with dotted-dashed lines.

rapidity and in azimuthal angle and with a transverse momentum distribution proportional to

$$\exp\left[-\frac{k_\perp^2}{(0.45\ \text{GeV})^2}\right].$$

One is immediately struck by the increased clarity of the dip in the small-x part of the spectrum when θ_0 cuts are used. For example, for a jet energy of 150 GeV and $\theta_0=35°$, the peak of the distribution is predicted to be about 3 GeV. In this same situation at particle energies of 2 GeV the dip is already pronounced, while the estimated background contamination is quite small. It appears that Eq. (49), the sharpest criterion for the coherence dip when θ_0 cuts are used, should be testable at hadronic colliders.

VI. COHERENCE AND FINAL STATES IN DEEPLY INELASTIC SCATTERING

The parton model had its first great successes in explaining the scaling observed in deeply inelastic lepton-hadron scattering. Later, scaling violations were explained by the approach to asymptotic freedom dictated by QCD and became the first quantitative testing area of that theory. The spectrum of particles associated with a deeply inelastic scattering event has only recently begun to receive serious theoretical treatment (Marchesini and Webber, 1984; Ciafaloni, 1986, 1987; Dokshitzer *et al.*, 1986; Gribov *et al.*, 1987). In this final section of our paper we shall briefly summarize the present situation. Our discussion will follow that of Dokshitzer, Khoze, and Troyan (1986) and Gribov *et al.* (1987) and is based on the unpublished work of Gribov and three of the present authors (Yu.D., V.K., and S.T.).

Our main concern here will be with the spectrum of particles associated with small-x deeply inelastic events. As far as the structure functions themselves are concerned, the dominant small-x regime will be given by the graphs of Fig. 12. So long as final-state particles are not measured, these graphs, with the appropriate running couplings inserted, will give the leading double logarithmic terms for small-x behavior if one imposes $k_{1\perp}<k_{2\perp}<\cdots<k_n<Q$, which condition actually comes from interference effects (Bassetto *et al.*, 1983; Mitra, 1983). However, in order to calculate the single-particle spectrum it is not enough to consider simply those graphs shown in Fig. 12, even allowing that the horizontal parton lines shown there may fragment. Sets of graphs that cancel in the structure function calculation no longer cancel in the inclusive spectrum.

In general terms, we expect two distinct regions, or jets, to be produced. The quark line $q+k_n$ should form the current jet, while the remaining lines the target jet. The laboratory frame is not ideal in separating these two regions. A better frame is the Breit frame of k_n obtained by choosing

$$P=(\sqrt{P^2+M^2},0,0,P),\quad q=(0,0,0,-2xP)\ , \qquad (50)$$

in which case the current jet should be going along the negative z axis and have energy xP. The target jet travels along the positive z axis. The separation of the two different jets is now simply according to which direction the particles are going.

The final-state properties of particles in the current jet should be identical to those of jets produced in e^+e^- annihilation and in hard hadronic processes. This jet, line k_n+q in Fig. 12, is born at the instant of the hard-photon interaction and then evolves rather independently of the rest of the process. The target jet is quite complicated, and the single word "jet" is not perhaps completely appropriate. Particles traveling along the positive z axis, in our Breit frame, may come from decays of one of the "subjects" $k_1',\ldots,k_n'$, they may come from additional semihard emissions, to be discussed shortly, or they may come from fragmentation of the part of the target that is a spectator as far as hard interactions and evolution are concerned. That is, the target fragmentation region consists of both particles produced from hard interactions and those from soft interactions. Our discussion will focus on those particles produced from hard sources, that is from the evolution of the system toward the hard interaction initiated by q. Of course, identical target fragmentation jets occur in hadronic jet production when the transverse momentum of the hard scattering, $p_\perp$, obeys $p_\perp^2/s\ll 1$ and in μ-pair production when $Q^2/s\ll 1$.

The character of "soft" radiation associated with the hard scattering can be understood, to a large extent, by considering radiation from the elementary vertex $p\to k_1'+k_1$ appearing in Fig. 12 (Dokshitzer *et al.*, 1986). Suppose an additional gluon l is radiated from this vertex as shown in Fig. 13. We define $l_+=\beta_l+P_+$, $p_+=\beta_p P_+$, $k_{1+}=\beta_{k_1}P_+$, etc. We suppose $\beta_{k_1}\ll\beta'_{k_1}\approx\beta_p$, the usual strong ordering appropriate to small-x processes. Then there are two cases to consider: (i) $\beta_l<\beta_{k_1}$ and (ii) $\beta_l>\beta_{k_1}$.

(i) When $\beta_l<\beta_{k_1}$ there is of course radiation off $p\,(k_1')$

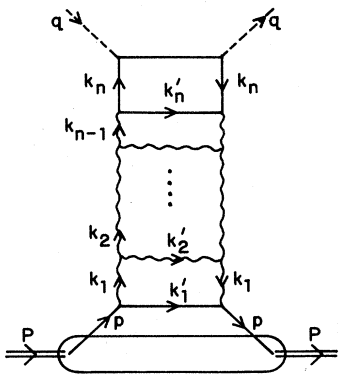

FIG. 12. Ladder graphs, with transverse momentum ordering, dominate in structure functions at small x.

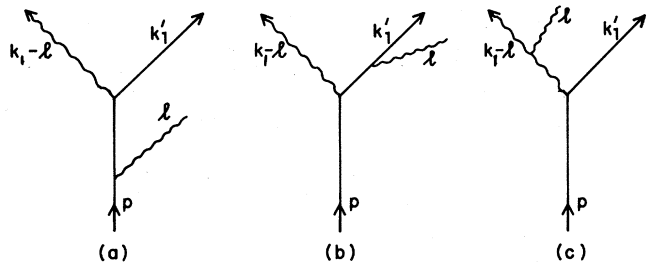

FIG. 13. Additional soft gluon l, radiated from the lower vertex of the graph shown in Fig. 12.

when $\theta_{pl}(\theta_{k_1'l})$ is less than $\theta'=\theta_{pk_1'}$, in the usual manner. The interesting region is $\theta_l \approx \theta_{lk_1'} \approx \theta_{lp} \gg \theta'$. Now when $2k_1 l < k_{1\perp}^2$, that is, when

$$\theta' < \theta_l < \frac{\beta_p}{\sqrt{\beta_{k_1}\beta_l}}\theta' , \tag{51}$$

the l line can be emitted off the p and k_1' lines coherently. When $2k_1 l > k_{1\perp}^2$ only the graph of Fig. 13(c) is effective, and here one covers the angular region

$$\theta' \frac{\beta_p}{\sqrt{\beta_{k_1}\beta_l}} < \theta_l . \tag{52}$$

However, the coherent emissions of Figs. 13(a) and 13(b) give the same answer in the region (51) as does the emission corresponding to Fig. 13(c) in region (52).

(ii) When $\beta_l > \beta_{k_1}$ it does not make sense to route the momenta as shown in Fig. 13. Rather, we should write the momenta for graphs (a) and (b) as shown in Fig. 14. Then so long as $l_\perp \ll k_{1\perp} \approx k_{1\perp}'$ these two graphs add coherently, that is, in the region

$$\theta_l < \frac{\beta_p}{\beta_l}\theta' . \tag{53}$$

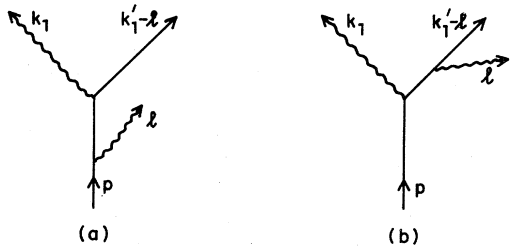

FIG. 14. Graphs that add coherently in region $l \gg k_1$.

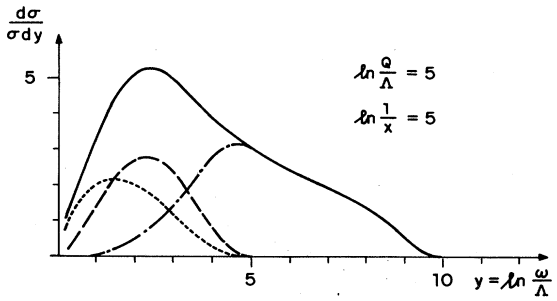

FIG. 15. Contributions to the energy particle spectrum in deeply inelastic scattering target fragmentation region at $\ln q/\Lambda = 5$, $\ln 1/x = 5$: Dotted curve (I), quark box contribution ; dashed curve (II), coherent "t-channel" color radiation; dotted-dashed curve (III), fragmentation of ladder rungs; solid curve, total sum.

The graph analogous to Fig. 13(c) is already included in Fig. 12, since here k_1 is the soft emission off l.

Thus the contributions to the inclusive spectrum are conveniently grouped into three parts. When $l < xP$ the line l is softer than all the lines appearing in Fig. 12. (Note we of course consider only the lines $p, k_1, k_1', \ldots, k_n, k_n'$ of Fig. 12. We are unable to discuss the true soft-hadron physics which would involve the lower blob of Fig. 12.) Then the discussion under (i) applies to emission off all lines in Fig. 12. There is a contribution, I, coming from emissions off the line k_n' when

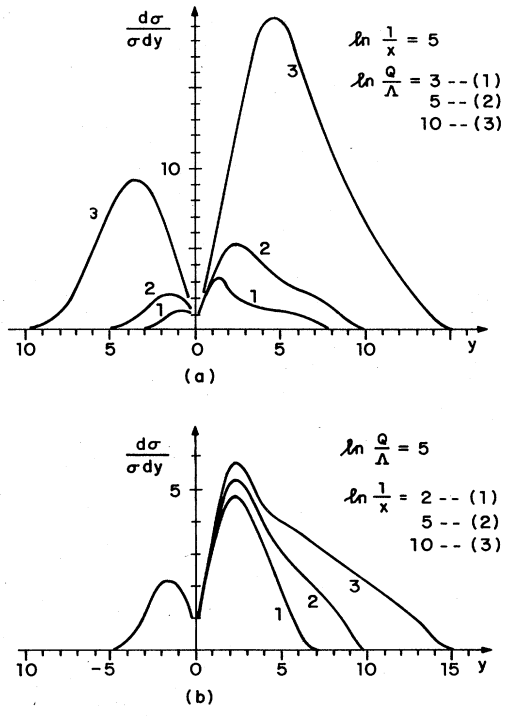

FIG. 16. Evolution of energy hadron distribution for deep-inelastic scattering in the Breit system with (a) q^2, $\ln q/\Lambda = 3$, 5, 10 at $\ln 1/x = 5$; and (b) x, $\ln 1/x = 2$, 5, 10 at $\ln q/\Lambda = 5$.

$\theta_{lk_n'} < \theta_{k_n'p}$, and off the line k_n when $\theta_{lk_n'} > \theta_{k_n'p}$. This contribution is

$$\left[\frac{d\sigma^h}{\sigma\, dy}\right]_{\rm I} = \frac{C_F}{N_c}\left[\frac{\omega}{xP}\bar{D}_g^h\left[\frac{\omega}{xP},\ln\frac{Q}{\Lambda}\right]\right], \tag{54}$$

with $y=\ln\omega/\Lambda$ and ω the energy of hadron h. Further, when $l < xP$ there is a contribution coming from effective emissions off the vertical gluon lines of Fig. 12. Iterating the argument under (i) these contributions are effective up to angles $\theta_{lp} < \theta'_{k_n}$ and give a contribution, II, as

$$\left[\frac{d\sigma^h}{\sigma\, dy}\right]_{\rm II} = \frac{1}{D_\beta^q(x,Q^2)}\int_0^{\ln Q/\Lambda} d\ln\frac{k_\perp}{\Lambda}\frac{\partial}{\partial\ln k_\perp/\Lambda}D_\beta^q(x,k_\perp^2)\left[\frac{\omega}{xP}\bar{D}_g^h\left[\frac{\omega}{xP},\ln\frac{k_\perp}{\Lambda}\right]\right] \tag{55}$$

with D_β^q the sea quark distribution of particle P.

Finally, when $xP < l < P$, case (i) applies only to some lower part of the ladder. Combining this region with the region (53) and also with normal emission off the rungs of the ladder in Fig. 12, one finds

$$\left[\frac{d\sigma^h}{\sigma\, dy}\right]_{\rm III} = \frac{1}{D_\beta^q(x,Q^2)}\int_{xP}^{P}\frac{dl}{l}\int^{\xi_Q} d\xi_k D_\beta^q\left[\frac{l}{P},k_\perp^2\right]\frac{\partial^2}{\partial\xi_k^2}D_g^q\left[\frac{xP}{l},Q^2,k_\perp^2\right]\int_\Lambda^{k_\perp}\frac{dl_\perp}{l_\perp}\frac{\alpha(l_\perp^2)}{2\pi}\left[\frac{\omega}{l}\bar{D}_g^h\left[\frac{\omega}{l},\ln\frac{l_\perp}{\Lambda}\right]\right] \tag{56}$$

with $\xi_k = 1/b\,\ln\ln k_{\perp/\Lambda}$.

In Fig. 15, we show the relative sizes of I, II, and III (Dokshitzer *et al.*, 1986), while in Fig. 16 the current fragmentation region is added in order to show the full hadronic distribution due to gluon emission. Unfortunately, we do not yet know how to give a good estimate of the soft hadronic background. This last point is very important in determining whether the striking dip shown, at $y=0$, in Fig. 16 will stand out. We believe that the soft-hadron background should not be strongly Q^2 dependent, so that the rapid $1/\sigma d\sigma/dy$ versus Q^2 shown in Fig. 16(a) should be visible, at least at HERA.

ACKNOWLEDGMENTS

Part of this work was done when one of the authors (A.M.) was a guest in the USSR. He wishes to thank the USSR Academy of Science, the Leningrad Nuclear Physics Institute, and ITEP for their hospitality during this visit. One of the authors (A.M.) wishes to thank Dr. R. K. Ellis for a number of helpful comments on the manuscript. This research was supported in part by the U.S. Department of Energy.

REFERENCES

Aihara, M., *et al.*, 1986, Phys. Rev. Lett. **57**, 945.
Althoff, A., *et al.*, 1984, Z. Phys. C **22**, 307.
Amati, D., and G. Veneziano, 1979, Phys. Lett. B **83**, 87.
Andersson, B., M. Bengtson, and G. Gustafson, 1982, "Fragmentation in the Lund model," Lund University Preprint No. LU-TP-82-10.
Andersson, B., G. Gustafson, G. Ingelman, and T. Sjostrand, 1983, Phys. Rep. **97**, 33.
Azimov, Ya. I., Yu. L. Dokshitzer, V. A. Khoze, and S. I. Troyan, 1985a, Z. Phys. C **27**, 65.
Azimov, Ya. I., Yu. L. Dokshitzer, V. A. Khoze, and S. I. Troyan, 1985b, Phys. Lett. B **165**, 147.
Azimov, Ya. I., Yu. L. Dokshitzer, V. A. Khoze, and S. I. Troyan, 1985c, *Materials of the XX Winter School of the Leningrad Nuclear Physics Institute* (Leningrad Nuclear Physics Institute, Leningrad), Vol. 1, p. 82.
Azimov, Ya. I., Yu. L. Dokshitzer, V. A. Khoze, and S. I. Troyan, 1986a, Z. Phys. C **31**, 213.
Azimov, Ya. I., Yu. L. Dokshitzer, V. A. Khoze, and S. I. Troyan, 1986b, Sov. J. Nucl. Phys. **43**, 95.
Azimov, Ya. I., Yu. L. Dokshitzer, V. A. Khoze, and S. I. Troyan, 1987, "QCD portrait of hadronic jets," Leningrad Nuclear Physics Institute Preprint No. 1230.
Bartel, W., *et al.*, 1983, Z. Phys. C **21**, 37.
Bashan, C., L. Brown, S. Ellis, and S. Love, 1978, Phys. Rev. Lett. **41**, 1585.
Bassetto, A., M. Ciafaloni, and G. Marchesini, 1980, Nucl. Phys. B **163**, 477.
Bassetto, A., M. Ciafaloni, and G. Marchesini, 1983, Phys. Rep. C **100**, 201.
Bassetto, A., M. Ciafaloni, G. Marchesini, and A. H. Mueller, 1982, Nucl. Phys. B **207**, 189.
Chudakov, A. E., 1955, Isv. Akad. Nauk SSSR Ser. Fiz. **19**, 650.
Ciafaloni, M., 1986, in *Proceedings of the XXIII International Conference on High Energy Physics,* Berkeley, edited by S. C. Loken (World Scientific, Singapore), Vol. I, p. 1181.
Ciafaloni, M., 1987, CERN Publication No. CERN-TH-4672/87.
Dokshitzer, Yu. L., D. I. Dyakonov, and S. I. Troyan, 1978, Phys. Lett. B **78**, 290.
Dokshitzer, Yu. L., V. S. Fadin, and V. A. Khoze, 1982a, Phys. Lett. B **115**, 242.
Dokshitzer, Yu. L., V. S. Fadin, and V. A. Khoze, 1982b, Z. Phys. C **15**, 325.
Dokshitzer, Yu. L., V. S. Fadin, and V. A. Khoze, 1983, Z. Phys. C **18**, 37.
Dokshitzer, Yu. L., V. A. Khoze, and S. I. Troyan, 1986, "Coherence in high energy jets," Leningrad Nuclear Physics Institute Preprint No. 1218.
Dokshitzer, Yu. L., and S. Troyan, 1984, "Nonleading perturbative contributions to the dynamics of quark-gluon cascades and soft hadron spectra in e^+e^- annihilation," Leningrad Nuclear Physics Institute Preprint No. 922.

Eichten, E., I. Hinchliffe, K. Lane, and C. Quigg, 1984, Rev. Mod. Phys. **56**, 579.
Ellis, R. K., G. Marchesini, and B. R. Webber, 1986, Nucl. Phys. B **286**, 643.
Erdelyi, A., 1953, Ed., *Bateman Manuscript Project: Higher Transcendental Functions* (McGraw-Hill, New York).
Ermolaev, B. I., and V. S. Fadin, 1981, JETP Lett. **33**, 269.
Fadin, V. S., 1983, Yad. Fiz. **37**, 408.
Field, R. D., 1986, Nucl. Phys. B **264**, 687.
Gaffney, J., and A. H. Mueller, 1985, Nucl. Phys. B **250**, 109.
Gottschalk, T., 1985, "A backwards evolution Monte Carlo for initial state parton showers," California Institute of Technology Preprint No. CALT-68-1241.
Gribov, L. V., Yu. L. Dokshitzer, V. A. Khoze, and S. I. Troyan, 1987, JETP Lett., in press
Hanson, G., *et al.*, 1975, Phys. Rev. Lett. **35**, 1609.
Hofmann, W., 1986, in *Proceedings of the XXIII International Conference on High Energy Physics,* Berkeley, edited by S. C. Loken (World Scientific, Singapore), Vol. I, p. 1093.
Konishi, K., A. Ukawa, and G. Veneziano, 1979, Nucl. Phys. B **157**, 45.
Malaza, E. D., 1986, Z. Phys. C **31**, 143.
Malaza, E. D., and B. R. Webber, 1984, Phys. Lett. B **149**, 501.
Marchesini, G., and B. R. Webber, 1984, Nucl. Phys. B **238**, 1.
Marchesini, G., and B. R. Webber, 1987, private communication.
Mitra, N., 1983, Nucl. Phys. B **218**, 145.
Mueller, A. H., 1981, Phys. Lett. B **104**, 161.
Mueller, A. H., 1983, Nucl. Phys. B **213**, 85; **241**, 141(E).
Mueller, A. H., 1984, Nucl. Phys. B **228**, 351.
Paige, F. E., and S. Protopopescu, computer program ISAJET (unpublished).
Saxon, D., 1986, *Proceedings of the European Physical Society Meeting on High Energy Physics,* Bari, Italy, 1986 (European Physical Society, Geneva), p. 901.
Sheldon, P. D., *et al.*, 1986, Phys. Rev. Lett. **57**, 1398.
Sjostrand, T., 1985, Phys. Lett. B **157**, 321.
Sjostrand, T., 1986, Comput. Phys. Commun. **39**, 347.
Sugano, K., 1986, "Gluon jets," Argonne National Laboratory Report No. ANL-86-133.
Webber, B. R., 1984, Nucl. Phys. B **238**, 492.
Yamamoto, H., 1985, in *International Symposium on Lepton and Photon Interactions at High Energies (12th),* Kyoto, edited by Michiji Konuma and Kasuke Takahashi (Kyoto University, Kyoto), p. 50.